J Therm Anal Calorim (2015) 122:1485–1491
DOI 10.1007/s10973-015-4864-x

Kinetic study of the removal of pure and mixed $TTMA^+$, $CTMA^+$ and $DTMA^+$ templates from MCM-41

Cíntia C. Costa[1] · Dulce M. A. Melo[2] · Maria S. B. Fontes[5] · Joana M. F. Barros[3] · Marcus A. F. Melo[4] · Antonio E. Martinelli[5]

Received: 20 January 2015 / Accepted: 13 June 2015 / Published online: 2 July 2015

Abstract This work assessed the thermal degradation of surfactants, i.e., tetradecyltrimethylammonium bromide ($TTMA^+$—$C_{17}H_{38}NBr$), cetyltrimethylammonium bromide ($CTMA^+$—$C_{19}H_{42}NBr$) and trimethyloctadecylammonium bromide ($DTMA^+$—$C_{21}H_{46}NBr$), used to obtain MCM-41-type mesoporous materials using Flynn–Wall kinetic model. The cationic surfactants and their mixture at ratios of 1:1 and 1:1:1 resulting materials were labeled C_{17}, C_{19}, C_{21}, $C_{17}C_{19}$, $C_{19}C_{21}$, $C_{17}C_{21}$ and $C_{17}C_{19}C_{21}$. Before the kinetic study, the materials obtained by the hydrothermal method were characterized by physical, chemical and microstructural analyses such as X-ray diffraction (XRD), Fourier transform infrared spectroscopy, thermogravimetric and nitrogen adsorption–desorption plots (BET). The mesoporous materials showed a well-defined hexagonal arrangement from the calcination process and significant structural differences. The kinetic model was used to determine the apparent activation energy for the removal of pure surfactant and associated with pores of the MCM-41-type molecular sieve. From the kinetic study results, a decrease in activation energy was observed when using the mixture of surfactants, especially $C_{17}C_{19}$. Combining these results with XRD and BET analyses, it was observed that $C_{17}C_{19}$ showed the largest surface area and pore volume along with hexagonal arrangement. The mixture of cationic surfactants of hydrophobic chains of different sizes used in the preparation of MCM-41 reduced the activation energy and surfactant removal.

Keywords MCM-41 · Kinetics · $TTMA^+$ · $CTMA^+$ and $DTMA^+$

Introduction

The development of mesoporous materials of the MCM-41 family by researchers at Mobil Oil Corporation (USA) was a milestone in the synthesis of materials. New synthesis routes are still under development for directional applications [1, 2]. Due to its versatility and simple preparation, MCM-41 has significantly contributed to the areas of catalysis [3], adsorption [4, 5], energy [6] and biomedical research [7], among others.

The key parameters in the synthesis of MCM-41 are gel composition, type and size of the surfactant chain, pH, temperature and synthesis time. Surfactant molecules play an important role in the generation of porosity in solid materials. MCM-41 was originally synthesized under alkaline conditions where anionic inorganic species (I^-) are stabilized with cationic surfactants (S^+) by strong interactions (S^+I^-) [2, 3]. After the synthesis, surfactant molecules occluded in the pores must be removed, which can be achieved by ultrasound [8], supercritical fluid [9], ozone [10], plasma [11] or microwave [12]. Nevertheless, calcination is the most widely used approach to remove

✉ Cíntia C. Costa
natcintia@gmail.com

1 NUPRAR, Federal University of Rio Grande do Norte, Natal, RN 59072-970, Brazil

2 Chemical Institute, Federal University of Rio Grande do Norte, Natal, RN 59072-970, Brazil

3 Center of Education and Health, Federal University of Campina Grande, Cuité, PB 58175-000, Brazil

4 Department of Chemical Engineering, Federal University of Rio Grande do Norte, Natal, RN 59072-970, Brazil

5 Department of Materials Engineering, University of Rio Grande do Norte, Natal, RN 59072-970, Brazil

surfactants. In this study, the synthesis of MCM-41 mesoporous materials was performed with different cationic surfactants, alkyltrimethylammonium bromide ($C_nH_{2n}+1$ $N(CH_3)_3Br$, $n = 14$, 16 and 18), and the calcination process was used to remove the surfactants from the pores of MCM-41.

The formation of pores in a solid material usually requires the use of an organic template. Work has been carried out using long-chain organic surfactant molecules as structure-directing agent (SDA) during the synthesis of highly ordered mesoporous MCM-41 [2, 3]. Mixing cationic surfactants in the synthesis of MCM-41 is an innovation to optimize the formation of a mesoporous material and to tailor it according to different applications. The main advantages to use MCM-41 include its hexagonal structure, unidimensional pore structure, tailored pore size and reproducible surface properties [18]. This class of material has been widely studied due its simple preparation with negligible pore-networking and pore-blocking effects [1, 18]. Whereas MCM-41 has mainly been synthesized by $C_{19}H_{42}NBr$ as surfactant [1, 19], the synthesis of MCM-41 reported herein depicted very good hexagonal structure (p6 m) using mixed surfactants with different alkyl chain lengths.

The silica–tensoactive interaction occurs at different levels in the materials, due to the determination of different activation energies involved in the process of SDA removal, from the pores of mesoporous materials. In the present kinetic study, the activation energies obtained from thermogravimetric analyses are used to assess the kinetic parameters for the removal of $TTMA^+$, $CTMA^+$ and $DTMA^+$ surfactants and their mixtures ($TTMA^+$ and $CTMA^+$ in the ratio of 1:1), ($TTMA^+$ and $DTMA^+$ in the ratio of 1:1), ($CTMA^+$ and $DTMA^+$ in the ratio of 1:1) and ($TTMA^+$ and $CTMA^+$ and $DTMA^+$ in the ratio of 1:1:1). The apparent activation energy required to remove the surfactants and their mixtures during the thermal conversion was evaluated according to Flynn and Wall model [13].

Experimental

Synthesis of MCM-41

Mesoporous MCM-41 materials were synthesized by the hydrothermal method using tetraethylorthosilicate (TEOS) as source of silica, sodium silicate, water and three surfactants of different chain sizes as template [14]. The surfactants used were: tetradecyltrimethylammonium bromide—C_{17} ($C_{17}H_{38}NBr$), cetyltrimethylammonium bromide—C_{19} ($C_{19}H_{42}NBr$) and trimethyloctadecylammonium bromide—C_{21} ($C_{21}H_{42}NBr$). Their mixtures were used in the following ratios: 1:1 of $C_{17}C_{19}$ ($C_{17}H_{38}NBr$+ $C_{19}H_{42}NBr$), 1:1 of $C_{17}C_{21}$ ($C_{17}H_{38}NBr$+ $C_{21}H_{42}NBr$), 1:1 of $C_{19}C_{21}$ ($C_{19}H_{38}NBr$+ $C_{21}H_{42}NBr$) and 1:1:1 of $C_{17}C_{19}C_{21}$ ($C_{17}H_{38}NBr$+ $C_{19}H_{38}NBr$+ $C_{21}H_{42}NBr$). The stoichiometric calculation was done for each surfactant individually, using the gel with molar composition: 4 SiO_2: 1 ($C_nH_{2n}+1$ $N(CH_3)_3Br$: 1 Na_2O: 200 H_2O). The gel was inserted in a Teflon autoclave and incubated for a period of 120 h at 373 K. The pH was daily adjusted to 9–10 using 30 % acetic acid. The materials obtained were filtered, washed and dried at 373 K for 3 h, and calcined at 823 K for 2 h under nitrogen followed by air [15]. After calcination, the materials were characterized by XRD, FTIR, BET and TG.

Characterization

The calcined samples were characterized by X-ray diffraction (XRD) on a XRD-6000 Shimadzu equipment operating at 30 kV and 30 mA with monochromatic CuKα radiation ($\lambda = 1.5406$ Å). Data were collected in the 2θ range from 1° to 10°, and 0.02° step.

The N_2 adsorption/desorption isotherms at 77 K were obtained from ASAP 2020 equipment (Micromeritics) and analyzed using the BET and BJH models to calculate specific surface and pore distribution, respectively.

Thermogravimetric analyses (TG/DTG) of materials under study were carried out in a model TGA/SDT Q600 thermobalance (TA Instruments) with heating rates of 5, 10 and 20 °C min^{-1} between 25 and 700 °C. The mass of the samples was approximately 3 mg, and dynamic nitrogen flowing at 100 mL min^{-1} was used as atmosphere.

Absorption spectroscopy analyses in the infrared region were performed in a Shimadzu IR Prestige spectrometer, using KBr as dispersing agent. Pellets were prepared by mixing approximately 0.7 mg of sample with an appropriate amount of KBr to reach concentration of 1 % by mass. The material obtained was homogenized and hydraulically pressed under 8 ton. Absorption spectra of MCM-41 samples were obtained in the mid-infrared region in the range from 400 to 4000 cm^{-1} with resolution of 4 cm^{-1}.

The Flynn–Wall model was used to determine the kinetic parameters for the decomposition of $TTMA^+$, $CTMA^+$ and $DTMA^+$ surfactants and their mixtures at ratios of 1:1 and 1:1:1. This method requires different heating rates, β, and the least squares method (linear regression) to determine the slope, $\Delta (\log \beta)/\Delta (1/T)$ [13].

The method considers that the activation energy of a certain material at a given mass loss (conversion) is proportional to $\Delta (1/T)$, in which a linear dependence is observed between the inverse of the absolute temperature in a certain percentage of mass loss, $1/T$, with respect to the logarithm of the heating rate, $\Delta (\log \beta)$.

$$E_a = -\left(\frac{R}{b}\right) \times \frac{\Delta \log \beta}{\Delta(1/T)} \quad (1)$$

Equation 1 shows the estimated activation energy (E_a) using the slope value Δ (log β)/Δ (1/T) and estimated b value around 0.457 for the first iteration. This is an iterative method using tabulated values for β interactions. These values have been determined and tabulated by Doyle [16] and comprises a range of $7 \leq E/RT \leq 60$ [17, 18].

Results and discussion

Figure 1 shows the X-ray diffraction pattern of C_{17}, C_{19}, C_{21}, $C_{17}C_{19}$, $C_{17}C_{21}$, $C_{19}C_{21}$ and $C_{17}C_{19}C_{21}$ samples. It was observed that all samples showed characteristic profiles of MCM-41 with the presence of the main diffraction peaks of the hexagonal mesoporous phase corresponding to planes (100), (110) and (200). It was also observed that materials containing the mixture of surfactants occluded in the pores showed higher peak intensity, especially $C_{17}C_{19}$. Interestingly, the surfactant of longest hydrophobic chain $DTMA^+$ used in the synthesis of C_{21} showed the lowest intensity in the diffraction peaks and contributed to the reduction in diffraction peaks of $C_{17}C_{21}$, $C_{19}C_{21}$ and $C_{17}C_{19}C_{21}$ mixtures. Selvam et al. [19] reported that surfactants of high molecular weight ($\geq C_{18}$) are of difficult solubilization, which could be the reason for the behavior of C_{21} sample.

Table 1 shows the adsorption parameters of C_{17}, C_{19}, C_{21}, $C_{17}C_{19}$, $C_{17}C_{21}$, $C_{19}C_{21}$ and $C_{17}C_{19}C_{21}$ samples. The specific surface area and pore distribution were determined by BET [20] by BJH models, respectively [21]. It was observed that the larger the size of the surfactant chain, the bigger the size of the pores. However, when surfactants of different chain sizes were mixed, the pore size is typically the average among those of the surfactants used.

Another aspect to be considered is that $C_{17}C_{19}$, which showed highest XRD peaks (Fig. 1), was the one that stood out in the adsorption parameters presented in Table 1, with largest surface area and pore volume.

Table 1 Adsorption parameters of materials

Samples	$S^a_{BET}/m^2\ g^{-1}$	a^b_0/nm	Dp^c/nm	$Vp^d/cm^3\ g^{-1}$	Tw^e/nm
C_{17}	1014	4.34	2.66	0.77	1.67
C_{19}	840	4.68	3.21	0.87	1.47
C_{21}	723	4.89	3.49	0.83	1.39
$C_{17}C_{19}$	1039	2.924	2.92	1.027	1.02
$C_{17}C_{21}$	772	3.207	3.20	0.72	0.72
$C_{19}C_{21}$	723	3.021	3.02	0.67	0.67
$C_{17}C_{19}C_{21}$	935	3.13	3.13	0.95	0.95

[a] BET surface area

[b] Hexagonal unit cell ($a_0 = 2d_{100}/\sqrt{3}$)

[c] Pore diameter calculated by BJH model

[d] Pore volume

[e] Pore wall thickness ($T_w = a_0 - d_{BJH}$)

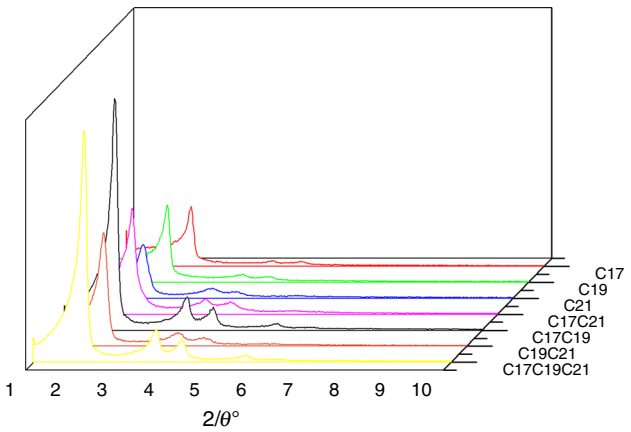

Fig. 1 XRD pattern of C_{17}, C_{19}, C_{21}, $C_{17}C_{19}$, $C_{17}C_{21}$, $C_{19}C_{21}$ and $C_{17}C_{19}C_{21}$ MCM-41 samples calcined at 550 °C

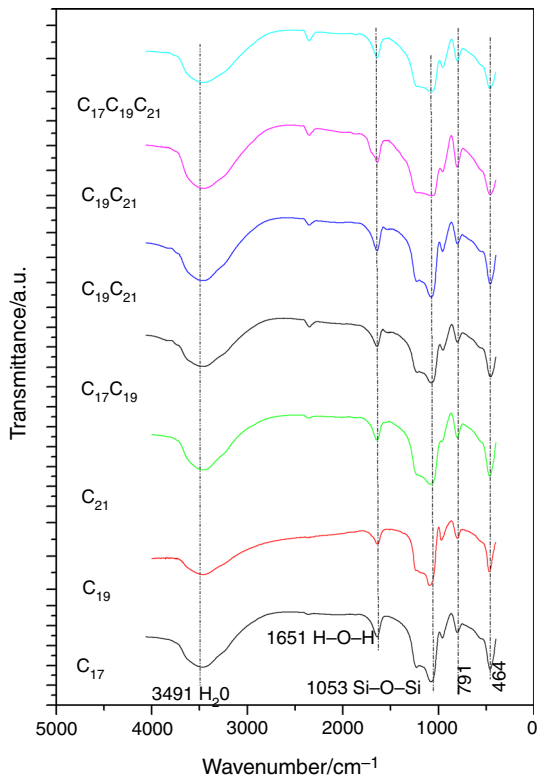

Fig. 2 FTIR patterns of C_{17}, C_{19}, C_{21}, $C_{17}C_{19}$, $C_{17}C_{21}$, $C_{19}C_{21}$ and $C_{17}C_{19}C_{21}$ calcined samples

Figure 2 illustrates the primary vibrational frequencies and their respective functions found in the materials studied. There was no stretching in the C–H bond of CH_2 and CH_3 groups of $TTMA^+$, $CTMA^+$ and $DTMA^+$ templates used in the formation of MCM-41 samples. This confirms the efficiency of the calcination process [22].

Figure 3 shows the TG/DTG plots of C_{17}, C_{19}, C_{21}, $C_{17}C_{19}$, $C_{17}C_{21}$, $C_{19}C_{21}$ and $C_{17}C_{19}C_{21}$ non-calcined samples obtained with heating rates of 5, 10 and 20 °C/min^{-1}. There were three mass-loss characteristics of MCM-41-type mesoporous materials. The first one is related to the loss of adsorbed water, the second one to the decomposition of surfactants occluded in the pores and the third mass-loss event to the condensation of silanol groups of the internal pore surface [23]. Table 2 shows the temperature ranges and the respective mass losses related to the decomposition of surfactants. The TG/DTG (Fig. 3) analyses showed degradation in the lower temperature range of the samples containing mixtures of surfactants occluded in the pores of MCM-41. Costa et al. [25] observed from the TG/DTG profile of MCM-41 with different lengths and

Table 2 Temperature range used in the kinetic study of samples

Samples	Range of temperature/°C	Mass loss/%
C_{17}	165–318	18.30
C_{19}	176–326	26.11
C_{21}	179–323	43.53
$C_{17}C_{19}$	243–323	11.39
$C_{17}C_{21}$	216–352	13.72
$C_{19}C_{21}$	218–342	22.40
$C_{17}C_{19}C_{21}$	222–336	10.95

observed that the mass loss profile increased with the surfactant chain length. Longer surfactant chains use more space inside the pores. Similar results were observed herein.

Figure 4 shows the distribution of the apparent activation energy involved in the removal of templates as a function of the degree of conversion of the synthesized samples. It was observed that the apparent activation energy varied depending on the surfactant used in the preparation of

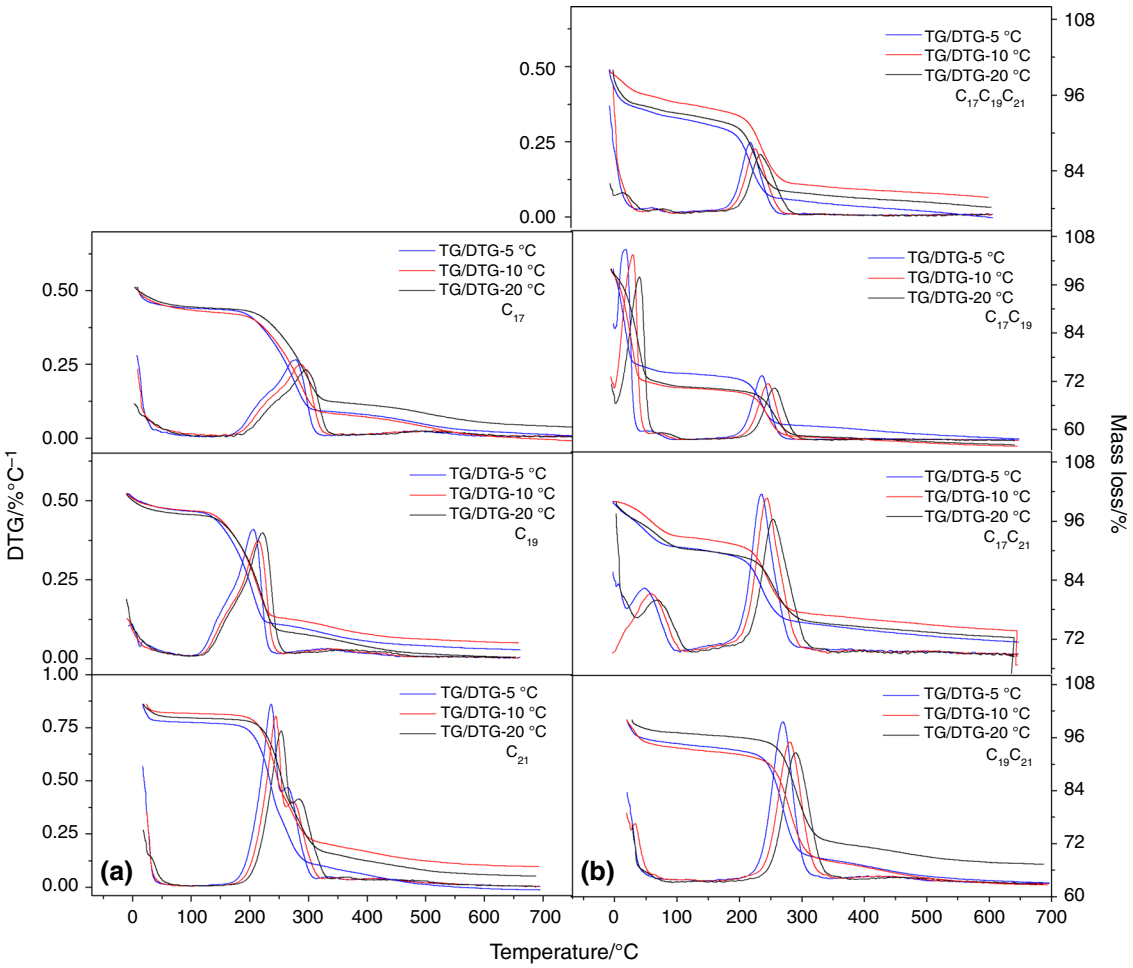

Fig. 3 TG plots of C_{17}, C_{19}, C_{21}, $C_{17}C_{19}$, $C_{17}C_{21}$, $C_{19}C_{21}$ and $C_{17}C_{19}C_{21}$ non-calcined samples at different heating rates: 5, 10 and 20 °C

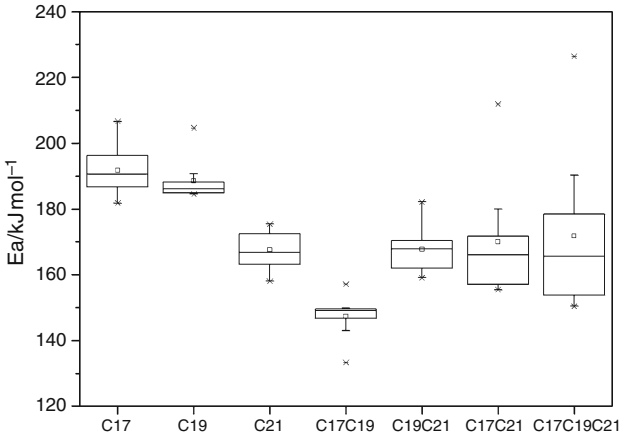

Fig. 4 Statistical distribution of the apparent activation energy for the removal of $TTMA^+$, $CTMA^+$ and $DTMA^+$ from C_{17}, C_{19}, C_{21}, $C_{17}C_{19}$, $C_{17}C_{21}$, $C_{19}C_{21}$ and $C_{17}C_{19}C_{21}$ samples

MCM-41. The activation energy decreased considerably as the hydrophobic chain of the surfactant increased in the following order: $TTMA^+ > CTMA^+ > DTMA^+$, i.e., larger hydrophobic chains form larger micelles with larger empty space between them. The reduction in the apparent activation energy can be associated with the heat diffusion and mass transfer for the removal of $DTMA^+$ surfactant occluded in the pores of MCM-41. Comparing materials synthesized with pure surfactants with those synthesized with mixtures of surfactants at ratios of 1:1 and 1:1:1, it could be observed a decrease in the average apparent activation energy of material synthesized with mixture of surfactants, especially in the $C_{17}C_{19}$ sample. The material with largest pore volume ($C_{17}C_{19}$) has more empty spaces among its pores, decreasing the silica–tensoactive interaction, thus resulting in a lesser need of energy to be removed. This fact may be associated with the process of micelle formation when a mixture of surfactants of different hydrophobic chains is used. In this case, the formation of micelles of various sizes may have occurred, increasing the empty space between them and facilitating the transfer of heat and mass, making the diffusion process quicker and requiring less energy. This fact can also be observed in TG/DTG (Fig. 3), where plots exhibit lower temperature range of degradation in samples with mixture of surfactants occluded in the pores of MCM-41.

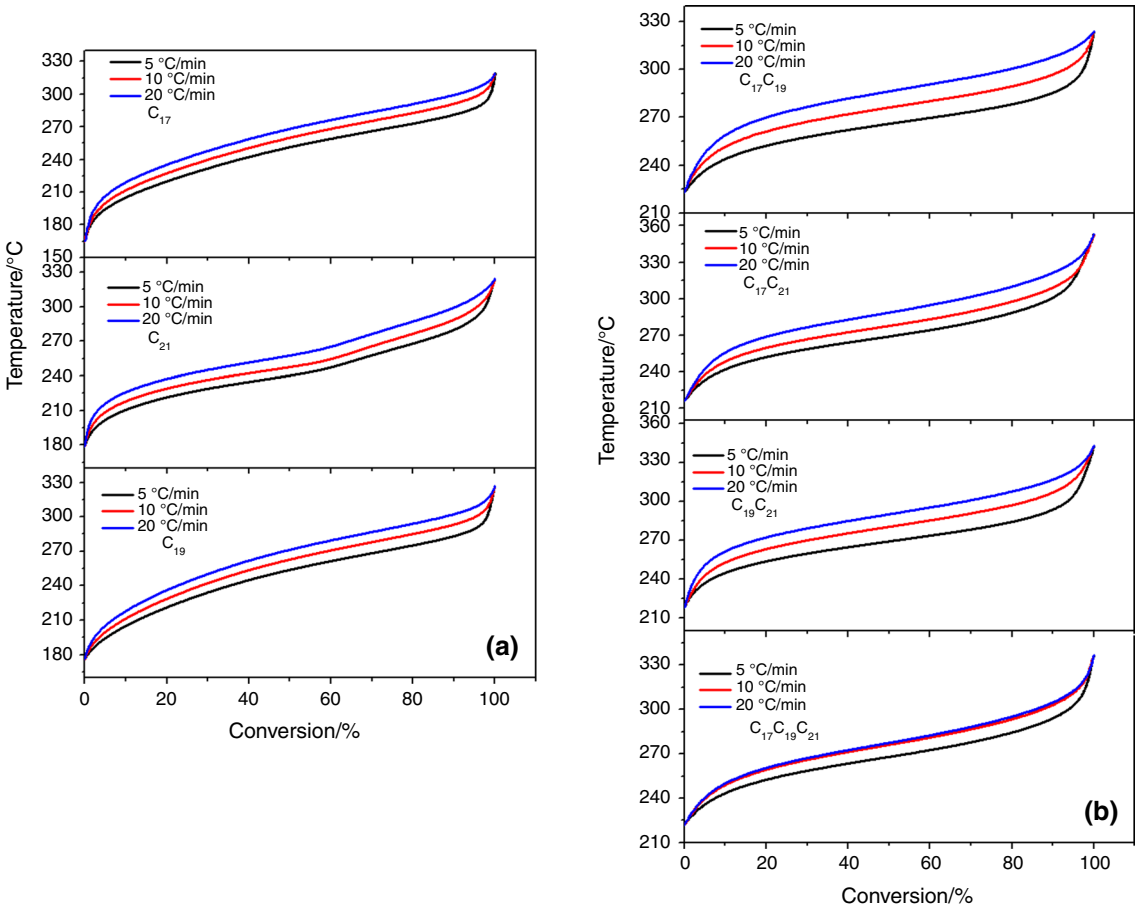

Fig. 5 Conversion *curves* as a function of temperature of C_{17}, C_{19}, C_{21}, $C_{17}C_{19}$, $C_{17}C_{21}$, $C_{19}C_{21}$ and $C_{17}C_{19}C_{21}$ samples

Another aspect to be considered is that the sample with the lowest apparent activation energy, $C_{17}C_{19}$, was the one that stood out in terms of surface area, pore volume, hexagonal arrangement and activation energy. The mixture of surfactants $TTMA^+$ and $CTMA^+$ used in the preparation of MCM-41 contributed to the synthesis of a material with optimized characteristics.

Figure 5 shows the conversion versus temperature plots measured by thermogravimetric analyses at heating rates of 5, 10 and 20 °C min^{-1} obtained by Eq. 2:

$$\propto = \frac{(m_0 - m_t)}{(m_0 - m_f)} \quad (2)$$

where α is the conversion, m_0 is the initial sample mass, m_f is the final sample mass, and m_t is the sample mass that varies with temperature.

It can be seen from Fig. 5 that gradually heating the material at 5 °C/min resulted in conversion to nearly full extent for all samples. Moreover, for the same heating rate, lower conversion temperatures were noticed for samples synthesized using mixtures of surfactants compared with those prepared using a single surfactant. The presence of mixture of surfactants in the MCM-41 favors minor apparent activation energy values for template removal from the porous system of MCM-41 compared with MCM-41 synthesized with a single surfactant. Braga et al. [24] and Souza et al. [15] reported E_a values of 170 and 166 kJ mol^{-1}, respectively, for MCM-41 synthesized with $CTMA^+$. These values are high compared with that of E_a of $C_{17}C_{19}$ sample, i.e., 147 kJ mol^{-1}.

A possible explanation for this fact corresponds to the structure of MCM-41 itself. The hydrophilic component of the surfactant, which is positively charged, interacts with the surface of the pores of mesoporous MCM-41 materials via Coulomb forces. The apparent activation energy involved in the removal of $TTMA^+$, $CTMA^+$ and $DTMA^+$ located within the pores of the molecular sieves provides the magnitude of the interactions between the template and silica [24]. The different values of the activation energy for the removal of the template between plain and mixed surfactants to pores of MCM-41 suggest different chemical interactions. These results also imply an interaction of mixed surfactants contained in the MCM-41 structure species used in the MCM-41 synthesis acting toward removing the template.

Conclusions

MCM-41-type mesoporous materials obtained by the hydrothermal method using $TTMA^+$, $CTMA^+$ and $DTMA^+$ surfactants and their mixtures at ratios of 1:1 and 1:1:1 showed well-defined hexagonal arrangement after calcination. FTIR and XRD analyses confirmed the successful synthesis formation of MCM-41. The results of the kinetic study proposed by Flynn–Wall showed a decrease in the activation energy of MCM-41 samples synthesized with the mixture of surfactants, mainly in $C_{17}C_{19}$ sample. Combining these results with XRD and BET analyses, it was observed that the $C_{17}C_{19}$ sample showed largest surface area, pore volume and hexagonal arrangement, which suggests lower activation energy involved in the process of removal of this templates, since this material shows easier energy and mass diffusion.

Acknowledgements The authors gratefully acknowledge the Refine and Catalysis Laboratories (NUPRAR/LCR) at UFRN, the Post-Graduation Programs in Petroleum Science and Engineering and Materials Science and Engineering (PPGCEP/PPGCEM) and CAPES (Improve Coordination of Superior Academic Level People) for the financial support and scholarship provided.

References

1. Meynen V, Cool P, Vansant EF. Verified syntheses of mesoporous materials. Microporous Mesoporous Mater. 2009;125:170.
2. Pal N, Bhaumik A. Soft templating strategies for the synthesis of mesoporous materials: inorganic, organic–inorganic hybrid and purely organic solids. Adv Colloid Interface Sci. 2013;21:189–90.
3. Galo JAA, Soler I, Sanchez C, Lebeau B, Patarin J. Chemical strategies to design textured materials: from Microporous and Mesoporous oxides to nanonetworks and hierarchical structures. Chem Rev. 2002;102:4093.
4. Belmabkhout Y, Guerrero RS, Sayari A. Adsorption of CO_2-containing gas mixtures over amine-bearing pore-expanded MCM-41 silica: application for CO_2 separation. Adsorption. 2011;17:395–401.
5. Kamarudin KSN, Alias N. Adsorption performance of MCM-41 impregnated with amine for CO_2 removal. Fuel Process Technol. 2013;106:332–7.
6. Xu W, Gao L, Wang S, Xiao G. Biodiesel production in a membrane reactor using MCM-41 supported solid acid catalyst. Bioresour Technol. 2014;159:286–91.
7. Popova M, Szegedi A, Yoncheva K, Konstantinov S, Petrova GP, Aleksandrov HA, Vayssilov GN, Shestakova P. New method for preparation of delivery systems of poorly soluble drugs on the basis of functionalized mesoporous MCM-41. Microporous Mesoporous Mater. 2014;198:247–55.
8. Jabariyan S, Zanjanchi MA. A simple and fast sonication procedure to remove surfactant templates from mesoporous MCM-41 Ultrason. Sonochem. 2012;19:1087–95.
9. Kawi S, Lai MW. Supercritical fluid extraction of surfactant from Si-MCM-41. AIChE J. 2002;48:1572–7.
10. Keene MTJ, Denoyel R, Lleewllyn PL. Ozone treatment for the removal of surfactant to form MCM-41 type materials. Chem Commun. 1998;20:2203.
11. Liu Y, Pan Y, Wang ZJ, Kuai P, Liu CJ. Facile and fast template removal from mesoporous MCM-41 molecular sieve using dielectric-barrier discharge plasma. Catal Commun. 2010;11:551–6.
12. Tian B, Lui X, Yu C, Gao F, Luo Q, Xie S, Tu B, Zhao D. Microwave assisted template removal of siliceous porous materials. Chem Commun. 2002;11:1186.

13. Flynn JH, Wall LA. A quick, direct method for the determination of activation energy from thermogravimetric data. Polym Lett. 1966;4:323–8.
14. Beck JS, et al. A new family of mesoporous molecular sieves prepared with liquid crystal templates. J Am Chem Soc. 1992;114:10834–43.
15. Souza MJB, Silva AOS, Aquino JMFB, Fernandes VJ Jr, Araújo AS. Kinetic study of template removal of MCM-41 nanostructured material. J Therm Anal Calorim. 2004;75:693–8.
16. Doyle CD. Kinetic analysis of thermogravimetric data. J Appl Polym Sci. 1962;5:285–92.
17. Aquino FM, Melo DMA, Santiago RC, Melo MAF, Martinelli AE, Freitas JCO, Araújo LCB. Thermal decomposition kinetics of PrMO3 (M = Ni or Co) ceramic materials via thermogravimetry. J Therm Anal Calorim. 2011;104:701–5.
18. Braga RM, Melo DMA, Aquino FM, Freitas JCO, Melo MAF, Barros JMF, Fontes MSB. Characterization and comparative study of pyrolysis kinetics of the rice husk and the elephant grass. J Therm Anal Calorim. 2013;115:1915.
19. Selvam P, Bhatia SK, Sonwane CG. Recent advances in processing and characterization of periodic. Ind Eng Chem Res. 2001;40:3237.
20. Brunauer S, Emmett PH, Teller E. Adsorption of gases in multimolecular layers. J Am Chem Soc. 1938;60:309.
21. Barrett EP, Joyner LJ, Halenda PP. The determination of pore volume and area distributions in porous substances I. Computations from nitrogen isotherms. J Am Chem Soc. 1951;73:373.
22. Flanigen EM, Khatami H, Szymanski HA. Molecular sieve zeolites. In: Flanigen EM, Sand LB, editors. Advances in chemistry series, vol. 101. Washington, DC: American Chemical Society; 1971.
23. Park M, Komarneni S. Adsorption breakthrough behavior: unusual effects and possible causes. Microporous Mesoporous Mater. 1998;25:75.
24. Braga RM, Barros JMF, Melo DMA, Melo MAF, Aquino FM, Freitas JCO, et al. Kinetic study of template removal of MCM-41 derived from rice husk ash. J Therm Anal Calorim. 2013;111(2):1013–8.
25. Costa CC, Melo DMA, Melo MAF, Mendoza ME, Nascimento JC, Andrade JM, et al. Effects of different structure-directing agents (SDA) in MCM-41 on the adsorption of CO_2. J Porous Mater. 2014;21(6):1069–77.